

Regenerator Friction Factor and Nusselt Number Information Derived from CFD Analysis

M.J. Cheadle, G.F. Nellis, S.A. Klein

University of Wisconsin Madison
Madison, WI 53703

ABSTRACT

Macroscopic models used in the design and development of pulse tube cryocooler regenerators do not explicitly consider the complex microscopic interaction of the working fluid as it flows through the interstitial passages formed by the solid matrix. Rather, the governing equations for these models are typically formulated in terms of average macroscopic quantities (e.g., the bulk velocity and temperature within the interstitial passage) and require user input in the form of friction factor and Nusselt number to account for microscopic fluid-to-solid interactions. Traditionally, the friction factor and Nusselt number are correlated from steady flow experimental data, despite the oscillatory flow that exists within the regenerator. It is not clear how well this technique works and how much the failure to account for oscillating flow affects the performance predicted by a macroscopic model of a regenerator. In addition, correlations from steady flow are limited in terms of the matrix configuration and the range of the conditions. This paper outlines the development of a design tool that is capable of deriving Nusselt number and friction factor correlations based on computational fluid dynamic (CFD) analysis of a unit-cell model that considers the microscopic interactions between the fluid and solid. The model explicitly includes the oscillating flow effects, can be applied to arbitrary matrix geometry, and can be used to provide information over a large range of operating conditions. This paper presents the details of the model and the data reduction process as well as preliminary results for a typical regenerator geometry.

INTRODUCTION

Like most real world problems, flow through a regenerator varies in all three dimensions as well as time. In addition, as depicted in Fig. 1, typical regenerator geometries are intricate porous structures with complex heat and momentum interactions at the fluid-solid interface. The REGEN3.3 model¹ developed at NIST formulates the numerical solution to the problem in terms of average cross-sectional quantities, thereby reducing the analysis to only one dimension rather than three. However, the microscopic heat and momentum interactions at the fluid-solid interface are not modeled directly using this approach. Instead, the details of the momentum and heat transfer interactions are included using friction factor and Nusselt number correlations. In the case of REGEN3.3, these correlations are taken from experimental data in Kays and London.² The correlations are limited in their range of applicability and no correlations exist for many geometries of interest. In

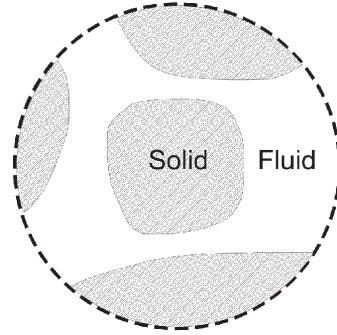


Figure 1. Arbitrary regenerator cross-section showing microscopic detail of the fluid-solid interface. Microscopic heat and momentum interactions in the cross-section are not modeled directly in the macroscopic model.

addition, the correlations are derived from steady state experimental data; their applicability to the oscillating flow conditions within the regenerator remains an open question. This paper details the development of a CFD model that has the potential to alleviate some of these problems. The detailed CFD model captures the heat and momentum interactions at the microscopic level and therefore can improve correlations by extending the range of existing correlations. The impact of oscillating flow can also be explicitly considered. Finally, the CFD model can be used to evaluate alternative porous structures such as micro-machined geometries.

REGEN GOVERNING EQUATIONS

Momentum Equation

The momentum conservation equation for the REGEN3.3 model is formulated in terms of average (across the channel at a given location and time) density, $\langle \rho \rangle$, average velocity, $\langle u \rangle$, and average pressure, $\langle P \rangle$.

$$\underbrace{\frac{\partial (\langle \rho \rangle \langle u \rangle)}{\partial t}}_{\text{momentum storage}} + \underbrace{\frac{\partial ((\langle \rho \rangle \langle u \rangle) \langle u \rangle)}{\partial x}}_{\text{momentum convection}} + \underbrace{\frac{\partial \langle P \rangle}{\partial x}}_{\text{pressure forces}} = \underbrace{\frac{\langle \rho \rangle u_\phi^2}{2D_h}}_{\text{momentum transfer}} f \quad (1)$$

Considering a control volume (CV), Eq. (1) balances momentum storage within the CV, with momentum convection into and out of the CV and pressure forces acting on the CV, the difference between these terms is represented with a momentum transfer term. This last term in Eq. (1) captures the microscopic momentum interactions between the fluid and the solid due to viscous forces and form drag. Notice that when steady, incompressible flow is considered, the first two terms in Eq. (1) are identically zero and the remaining terms can be rearranged to give the familiar definition of the friction factor:

$$f = \frac{\frac{\partial \langle P \rangle}{\partial x} D_h}{1/2 \langle \rho \rangle u_\phi^2} \quad (2)$$

where D_h is the hydraulic diameter and u_ϕ is the pore velocity.

A correlation for the friction factor, f , is a required input to REGEN3.3 that is currently derived from experimental data. One objective of this work is to numerically calculate the friction factor using the CFD model described subsequently.

Energy Equation

The energy conservation equation for the REGEN3.3 model is formulated in terms of the porosity, ϕ , cross-sectional area, A , average internal energy, $\langle e \rangle$, average enthalpy, $\langle h \rangle$, average conductivity, $\langle k \rangle$, and average temperature, $\langle T \rangle$.

$$\underbrace{\frac{\partial(\phi A \langle \rho \rangle \langle e \rangle)}{\partial t} + \frac{\partial(\phi A \langle \rho \rangle \langle u \rangle^2)}{\partial t}}_{\text{energy storage}} + \underbrace{\frac{\partial(\phi A \langle u \rangle \langle \rho \rangle \langle h \rangle)}{\partial x} + \frac{\partial(\phi A \langle u \rangle \langle \rho \rangle \langle u \rangle^2)}{\partial x}}_{\text{energy convection}} = \underbrace{-\frac{\partial}{\partial x} \left(\phi A \langle k \rangle \frac{\partial \langle T \rangle}{\partial x} \right)}_{\text{energy conduction}} = \underbrace{\frac{\phi A \langle k \rangle \langle \Delta T \rangle}{D_h \Delta x}}_{\text{heat transfer}} Nu \tag{3}$$

Equation (2) balances energy storage within the CV (both internal and kinetic) with energy convection into and out of the CV, with axial conduction into and out of the CV; the difference between these terms defines a heat transfer term. This last term in Eq. (3) captures the microscopic energy interactions between the fluid and the solid due to heat transfer to and from the fluid.

A correlation for the Nusselt number, Nu , is a required input to REGEN3.3 that is currently derived from experimental data correlations. A second objective of this work is to numerically calculate the Nusselt number using the CFD model described below.

CFD MODEL

Overview and Boundary Conditions

The idea behind the CFD analysis is to select a geometry for which friction factor and Nusselt number can be reasonably calculated. A geometric structure reducible to a unit-cell is optimal for minimizing computational memory and time. An overview of the selected geometry for the CFD model is shown in Fig. 2. Typical regenerator geometries are packed spheres or wire mesh screens. Modeling these geometries would require three-dimensional models with prohibitively long solution times. Instead, a simplified two-dimensional cylindrical array unit-cell was chosen for these preliminary results.

The two-dimensional unit-cell has several advantages, the most obvious being the reduced solution time when compared to a three-dimensional model. This is especially important when considering that the model will need to simulate oscillating flow. The staggered cylinder geometry is also advantageous in that it has similar flow characteristics to some commonly used regenerator geometries. Like packed spheres and mesh screens, at moderate Reynolds numbers a wake region will form downstream of each cylinder. The porosity, approximately 0.65, is similar to mesh screens. It also has directional similarity. This means that oscillating flow, as it moves from right to left, will encounter the same regenerator structure as when flow moves from left to right. Finally, the staggered cylinder array is a geometry that has been well studied. Because of its relative sim-

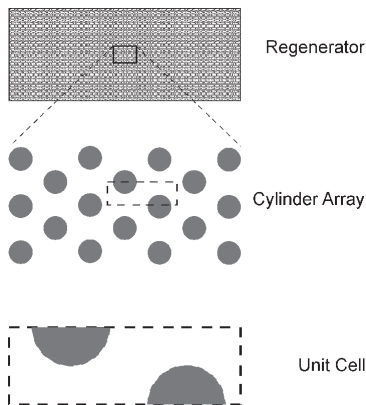


Figure 2. CFD model overview. The real regenerator geometry is modeled as two-dimensional staggered cylinder array unit-cell.

plicity and its use in heat exchangers and other applications, f and Nu have been measured ^{2,3} and these data can be compared to the numerical results.

The boundary conditions for the CFD model are shown in Fig. 3. The model is composed of nine unit-cells arranged in a series in order to avoid any end effects. For the momentum equation, spatially uniform velocity is specified on the left side boundary and allowed to vary in time to simulate oscillating flow. A constant, spatially uniform pressure is set at the right hand side. Symmetry boundaries are applied to fluid edges while no-slip conditions are applied to the cylinder surfaces. For the energy equation, similar to the momentum equation, symmetry boundary conditions are applied at fluid edges. The remaining boundary conditions for the energy equation, those on the left and right and along the cylinder walls, are constant temperature boundary conditions that form a decreasing linear temperature gradient from the left to the right. The left temperature boundary is set to 350 K (for entering fluid during half the cycle). For each succeeding unit cell a constant wall temperature 5 K less than the previous is applied. For example, unit-cell one is set to 345 K and unit-cell two is set to set to 340 K. At the right end, unit-cell nine is set to 305 K and the right boundary is set to 300 K (for entering fluid).

Fluent⁴ is used to solve the mass, energy, and full Navier-Stokes equations for incompressible flow with constant properties. Simulations were also run for compressible flows using the ideal gas equation used to calculate density; however the results were not significantly different than the results for incompressible flow. This can be attributed to the low flow speeds and small pressure changes across the unit-cells.

Model Calculations

There is a great amount of numerical information contained in the CFD results. In order to calculate the friction factor and Nusselt number from the simulation results it is necessary to formulate momentum and energy balances for the computational domain. The computations described below are carried out only for unit-cell five in order to avoid entrance effects.

An integral momentum balance for unit-cell five is given in Eq. (4):

$$\underbrace{\frac{d}{dt} \left(\int_A \rho \bar{u} dA \right)}_{\text{momentum storage}} + \underbrace{\int_{s_{out}} (\rho \bar{u}) (\bar{u} \cdot \bar{n}) ds - \int_{s_{in}} (\rho \bar{u}) (\bar{u} \cdot \bar{n}) ds}_{\text{momentum convection}} + \underbrace{\int_{s_{out}} \bar{P} \bar{n} ds - \int_{s_{in}} \bar{P} \bar{n} ds}_{\text{pressure forces}} = - \underbrace{\int_b (\bar{\tau} \cdot \bar{n}) ds}_{\text{viscous forces}} - \underbrace{\int_b \bar{P} \bar{n} ds}_{\text{form drag}} \quad (4)$$

where n is the outward-pointing unit normal along the boundaries, τ is the stress tensor, and ds is a differential boundary segment. The terms in Eq. (4) are numerically estimated by discretizing the integrals and using solution information from unit-cell five to quantify the individual terms in the equation. A comparison of the LHS of Eq. (4) to the LHS of Eq. (1) reveals that each term of Eq. (4) matches each term of Eq. (1), i.e. the terms in both equations are the momentum storage, momentum convection, and pressure forces. The difference of these terms, captured by the RHS, shows that the friction term, used in Eq. (1) to model the microscopic interactions of heat and momentum, is a result of viscous forces at the cylinder surface and form drag. Therefore, computation of the friction factor from the CFD results can be carried out in two ways: either by calculating the LHS or RHS of Eq. (4) and then multiplying by the appropriate scaling factor to obtain the dimensionless value of f . Both methods were used to calculate the friction factor results shown below and they agree quite well.

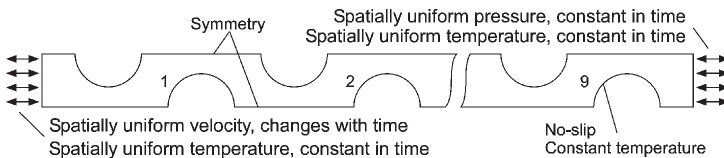


Figure 3. CFD model boundary conditions.

An integral energy balance for unit-cell five is given in Eq. (5):

$$\begin{aligned}
 & \underbrace{\frac{d}{dt} \int_A \rho u dA + \frac{d}{dt} \int_A \rho U^2 dA}_{\text{energy storage}} + \underbrace{\int_{s_{in}} \rho (h + U^2) \bar{u} \cdot \bar{d}s - \int_{s_m} \rho (h + U^2) \bar{u} \cdot \bar{d}s}_{\text{energy convection}} \\
 & + \underbrace{\int_{s_{in}} -k_g \bar{\nabla} T \cdot \bar{d}s - \int_{s_m} -k_g \bar{\nabla} T \cdot \bar{d}s}_{\text{energy conduction}} = \underbrace{\int_{s_{in}} \bar{q}'' \cdot \bar{d}s}_{\text{heat transfer}}
 \end{aligned} \tag{5}$$

Similar to the momentum equation, a comparison of terms on the LHS of Eq. (5) to terms on the LHS of Eq. (3) reveals similarity, i.e. both include terms for energy storage, energy convection and energy conduction. The difference is captured by the RHS heat transfer term which is the microscopic heat transfer between the fluid and the solid matrix. Like the friction factor, computations of the Nusselt number from the CFD simulations can be carried out by numerically integrating the LHS or RHS of Eq. (5) and multiplying by the appropriate scaling factor. Both methods were used to calculate the Nusselt number results and again, they agree quite well.

SIMILARITY PARAMETERS

It is convenient to correlate the calculated values of the friction factor and Nusselt number in terms of other similarity parameters so that they can be easily integrated into the REGEN3.3 model using a minimal number of simulations. Like most correlations of friction factor and Nusselt number, both the Reynolds number and the Prandtl number are used.

$$\text{Re} = \frac{u_\phi D_h}{\nu} \quad \text{Pr} = \frac{\mu C_p}{k} \tag{6}$$

where μ is the fluid viscosity and C_p is the heat capacity. In addition to these, the Valensi number is used:

$$Va = \frac{\omega D_h^2}{\nu} \tag{7}$$

where ω is the frequency of the oscillation. The Valensi number is the dimensionless frequency and can be thought of as a ratio of the hydraulic diameter to the momentum diffusion length. For example, at low frequencies momentum has ample time to penetrate across the hydraulic diameter many times over during a single cycle. Therefore the flow should have a fully developed boundary layer and behave in a quasi-steady manner at low values of Va . At high frequencies, the time available for the momentum to diffuse is reduced, eventually to the extent that it cannot penetrate to the center of the channel during a single cycle. The result is that the boundary layer is still developing when the fluid core begins to change directions. One would expect the partially developed boundary layer to have impact on the momentum and heat transfer at high Va .

RESULTS

Steady State Verification

Steady state CFD results for friction factor and Nusselt number as a function of Reynolds number for a Prandtl number of 1.0 are shown in Fig. 4 and Fig. 5, respectively. These results are compared to correlations for staggered cylinders presented in the Heat Exchanger Design Handbook (HEDH)³. Fig. 4 shows good agreement between the CFD calculated friction factor and the HEDH correlation from $Re = 3$ to 1000. In Fig. 4, the correlation is only shown down to $Re = 3$ because this is the limit of its range. However, the CFD model is not limited in this respect and is able to provide results well below $Re = 3$. This capability is advantageous because REGEN3.3 requires correlations to be evaluated for $Re \geq 0$ due to oscillating flow.

For Reynolds numbers greater than approximately 100, the Nusselt number results shown in Fig. 5 agree fairly well with HEDH correlation, which are taken from experimental correlations by

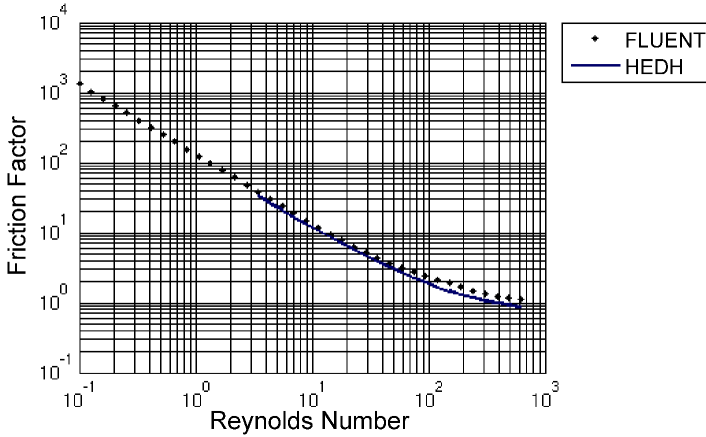


Figure 4. Friction factor as a function of Reynolds number for steady flow CFD calculations and HEDH experimental data correlations. $Pr = 1.0$.

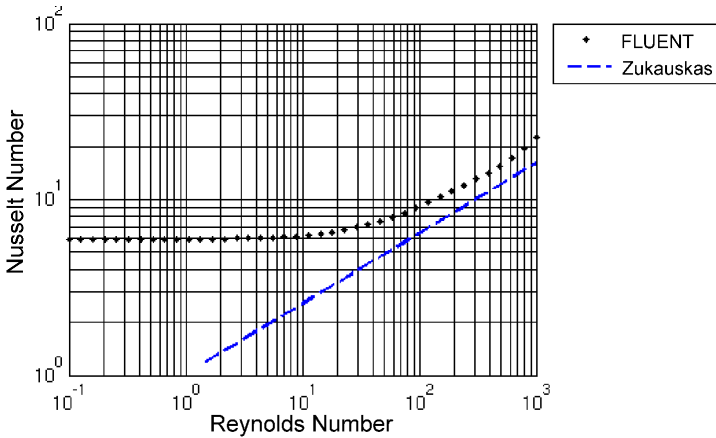


Figure 5. Nusselt number as a function of Reynolds number for steady flow CFD calculations and HEDH correlations based on experimental data of Zukauskas [5]. $Pr = 1.0$.

Zukauskas⁵. For $Re < 100$ the CFD calculations diverge from the correlations significantly. However, the Zukauskas correlation does not appear to be physical in its behavior in this range. One would expect the Nusselt number to reach a constant value at low Reynolds number. This is the behavior shown by the CFD calculations, which approach a constant value of approximately 6.0. The Zukauskas correlation, however, extrapolates to zero and its validity in this range is questionable. It may also be pointed out that the data used to generate the correlations are limited, particularly in the low Reynolds number range.

OSCILLATING FLOW RESULTS

Oscillating flow results for friction factor and Nusselt number are shown in Fig. 6 and Fig. 7, respectively. As can be seen in Fig. 6, friction factor is independent of Valensi number, for $Va < 10$, and is therefore not effected by oscillating flow in this range. For $Va > 10$, however, oscillating flow effects are evident. It is natural to compare these results to typical regenerator operating conditions. The Reynolds number and Valensi number for a regenerator with a hydraulic diameter of 20 mm, $\phi = 0.35$, oscillating at 60 Hz are estimated and shown in Fig. 6 and Fig. 7 based on the method presented in Cheadle, et al⁶. As flow moves from the warm end of the regenerator to the

cold end, the Valensi number and Reynolds number increase but, at least for this regenerator, never reach the region where oscillating flow effects become important. A similar plot for Nusselt number is shown in Fig. 7.

CONCLUSIONS

The CFD model developed in this paper is capable of numerically calculating friction factor and Nusselt number for a wide range of Reynolds, Prandtl, and Valensi numbers, beyond what is currently available with experimental data. It is capable of modeling steady state as well as oscillating flow and has been verified against previously existing correlations for staggered cylinder ar-

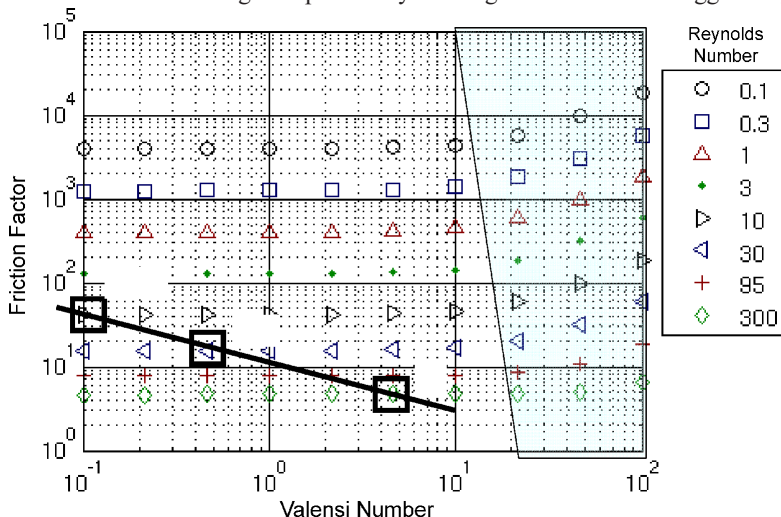


Figure 6. Friction factor as a function of Valensi number for various Reynolds numbers. The shaded region on the right hand side of the graph shows where oscillating flow effects begin to become important. The black, boxed line shows how Re, Va and friction factor change when moving toward the cold end of the regenerator for a 20 micron, packed sphere regenerator operating at 60 Hz with a porosity of 0.35.

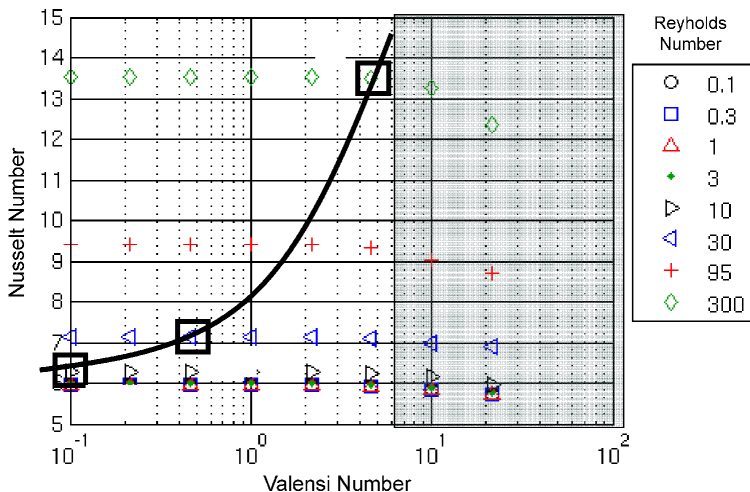


Figure 7. Nusselt number as a function of Valensi number for various Reynolds numbers. The shaded region on the right hand side of the graph shows where oscillating flow effects begin to become important. The black, boxed line shows how Re, Va and friction factor change when moving toward the cold end of the regenerator for a 20 micron, packed sphere regenerator operating at 60 Hz with a porosity of 0.35.

rays. Future work will entail improving correlations to existing geometries, developing correlations for new geometries, and integrating the results into REGEN3.3.

ACKNOWLEDGMENT

Financial support for this project was provided by the Office of Naval Research. Special thanks to Deborah Van Vechten.

REFERENCES

1. Gray, J., O’Gallagher, *REGEN3.3: User Manual*, National Institute of Standards and Technology, Boulder, CO, pp. 45-53.
2. Kays, W.M., and London, A.L., *Compact Heat Exchangers*, 3rd ed., Krieger Publishing Co., Malabar (1998).
3. Hewitt, G.F., ed., *Heat Exchanger Design Handbook*, Begell House, Inc., New York (2008).
4. *ANSYS FLUENT 12.0 Theory Guide*, (2009).
5. Wang, B., *Heat Transfer Science and Technology*, 1996. Higher Education Press, Beijing (1997), pp. 82-93.
6. Cheadle, M.J., Nellis, G.F., Klein, S.A., “Micro-Scale CFD Modeling of Oscillating Flow in a Regenerator,” *Adv. in Cryogenic Engineering*, Vol. 55, Amer. Institute of Physics, Melville, NY (2010), pp. 157-164.
7. Pfothhauer, J.M., Shi, J.L. and Nellis, G.F., “A Parametric Optimization of a Single Stage Regenerator Using REGEN 3.2,” *Cryocoolers 13*, Kluwer Academic/Plenum Publishers, New York (2005), pp. 463-470.